

Deuterium Experiments in the Sustained Spheromak Physics Experiment

*R.D. Wood, D.N. Hill, E.B. Hooper, H.S. McLean, D.D.
Ryutov, S. Woodruff*

This article was submitted to the 16th International Conference on
Plasma Surface Interactions

May 2004

U.S. Department of Energy

Lawrence
Livermore
National
Laboratory

DISCLAIMER

This document was prepared as an account of work sponsored by an agency of the United States Government. Neither the United States Government nor the University of California nor any of their employees, makes any warranty, express or implied, or assumes any legal liability or responsibility for the accuracy, completeness, or usefulness of any information, apparatus, product, or process disclosed, or represents that its use would not infringe privately owned rights. Reference herein to any specific commercial product, process, or service by trade name, trademark, manufacturer, or otherwise, does not necessarily constitute or imply its endorsement, recommendation, or favoring by the United States Government or the University of California. The views and opinions of authors expressed herein do not necessarily state or reflect those of the United States Government or the University of California, and shall not be used for advertising or product endorsement purposes.

This is a preprint of a paper intended for publication in a journal or proceedings. Since changes may be made before publication, this preprint is made available with the understanding that it will not be cited or reproduced without the permission of the author.

This report has been reproduced
directly from the best available copy.

Available to DOE and DOE contractors from the
Office of Scientific and Technical Information
P.O. Box 62, Oak Ridge, TN 37831
Prices available from (423) 576-8401
<http://apollo.osti.gov/bridge/>

Available to the public from the
National Technical Information Service
U.S. Department of Commerce
5285 Port Royal Rd.,
Springfield, VA 22161
<http://www.ntis.gov/>

OR

Lawrence Livermore National Laboratory
Technical Information Department's Digital Library
<http://www.llnl.gov/tid/Library.html>

P-362

Deuterium Experiments in the Sustained Spheromak Physics Experiment

R.D. Wood*, D.N. Hill, E. B. Hooper, H.S. McLean, D. Ryutov, S. Woodruff

Lawrence Livermore National Laboratory, Livermore, CA

Abstract

In this paper we report on the results of isotope exchange experiments in the Sustained Spheromak Physics Experiment (SSPX). We have compared ~500 deuterium discharges with similar discharges in hydrogen. Typically, we produce plasmas with peak toroidal currents in the range of 0.6 MA, electron temperatures (T_e) of ~200 eV and energy confinement times (τ_E) of ~200 μ s. The D₂ fueled discharges show similar results to those with H₂ fueling with no obvious differences in confinement time. Electron temperatures of ~200 eV with similar electron densities were observed. Both the deuterium and hydrogen fueled discharges have a calculated thermal conduction below $\chi_e < 10$ m²/s. However, the D₂ fueled discharges had a modest increase in high-Z (titanium) impurity content suggesting an increase of physical sputtering. We find no significant mass scaling effects.

Keywords: Deuterium, Impurities, Sputtering

R. D. Wood

7000 East Ave L-637

Livermore CA 94550

wood11@llnl.gov

1. Introduction

In this paper we discuss the results of fueling experiments with hydrogen and deuterium on the SSPX (Sustained Spheromak Physics Experiment) spheromak device. The SSPX is a magnetized coaxial gun-driven toroidal confinement device with plasma currents produced by the plasma dynamo rather than by external coils which link the vacuum vessel; this configuration offers the possibility of a less expensive fusion reactor. Analysis of previous spheromak experimental data [1,2] suggested that adequate core energy confinement could be obtained in these devices and that performance might scale favorably to power reactors. The SSPX device was built to explore spheromak confinement and current drive.

The spheromak plasma in SSPX is confined within an $R=1.0$ m, $h=0.5$ m, 1.2 cm thick conducting copper shell (flux conserver) which maintains the plasma shape due to image currents flowing in it. A cross section of the device is shown in Fig. 1; magnetic flux surfaces for an ideal MHD equilibrium computed with the CORSICA code [3] are included. The thin scrape-off layer region (less than 1 cm wide at the mid-plane) is connected to the electrode near the top of the injector. The gun-injected current of 200 kA produces plasmas with 600 kA of toroidal current and peak magnetic field (B_0) of ~ 1 T. The typical pulse length is 3.5 ms with peak $T_e > 200$ eV and $n_e = 0.7-1.0 \times 10^{20} \text{ m}^{-3}$.

Isotope scaling of transport is an important issue for magnetic fusion. Improvements in plasma performance, e.g. energy confinement time (τ_E), have been observed in tokamak discharges with deuterium fueling and a small, but reversed, effect in the ATF stellarator [4]. In tokamaks, the electron temperature is higher in deuterium-fueled discharges than in hydrogen. Many of the improvements in tokamak performance are attributed to changes in both the core and the edge/divertor properties that affect energy and particle transport.

In the remainder of this paper we present improved operation of the SSPX (Section 2), discuss surface conditioning, density control and gas inventory exchange in Section 3, and in Section 4 present results from deuterium fueled operations.

2. Improved spheromak operation

On SSPX the four phases of a discharge include breakdown, formation, sustainment, and decay. A time history of a typical discharge is shown in Figure 2. Fueling gas is puffed into the injector region $\sim 250 \mu\text{s}$ before connecting the high voltage formation bank. Breakdown occurs when the gas pressure in the injector region meets, or exceeds, the requirement for Paschen breakdown. Following breakdown, the plasma current (I_{gun}) in the injector region rises sharply for $\sim 100 \mu\text{s}$. When the increasing gun current reaches a threshold condition, the $\mathbf{J}\times\mathbf{B}$ force on the plasma in the injector accelerates, or ejects, it out of the injector into the flux conserver region to form the spheromak plasma. The ejection threshold condition occurs when the $\mathbf{J}\times\mathbf{B}$ pressure of the injector toroidal magnetic field becomes greater than the restoring force due to the injector radial bias magnetic flux (Φ_{gun}).

After breakdown and ejection of plasma into the flux conserver, if no additional energy is supplied, the spheromak disconnects from the injector and the current decays on a time scale consistent with resistive dissipation of the magnetic fields; these are formation only discharges. When additional energy is supplied from the sustainment bank via a pulse forming network that supplies constant current for $\sim 3 \text{ ms}$, the plasma can be sustained for a longer period of time. During the sustainment phase, the current from the gun drives reconnection processes that sustain and enhance the poloidal flux. Generally, the radiative losses are low and the decay is very gradual until the bank runs out of energy. As the gun current ramps down at the end of the discharge, the full duration discharges usually terminate abruptly due to MHD activity.

During spheromak formation, the poloidal field builds rapidly and is sustained by driving an instability of the open flux, a toroidal $n=1$ mode, which in turn provides fluctuations for a MHD dynamo to drive toroidal current. The $n=1$ mode provides the fluctuation power that couples current from the open flux into the spheromak. Higher order edge magnetic turbulence ($n=2,3,4$) then causes current to distribute throughout the spheromak and as a result the current in the core decays less rapidly than current at the edge. During sustainment excessive edge current and fluctuations degrade confinement. Optimal operation is obtained by flattening the profile of $\lambda=\mu_0 j/B$, consistent with reducing the drive for tearing and other MHD modes, and matching of edge current and bias flux to minimize $\delta B/B|_{\text{rms}}$. With these optimizations, the highest measured T_e (~ 250 eV, peaked at the magnetic axis) and lowest core thermal diffusivity ($\chi_e \sim 10\text{-}20$ m²/s) have been obtained.

3. Surface conditioning, density control and gas inventory exchange

To prevent sputtering of the copper conducting shell, the plasma facing surfaces are coated with a 100 μm thick layer of high-pressure plasma-sprayed (HPPS) tungsten. Characterization of the HPPS tungsten surface show interconnecting layers capable of absorbing high levels of water and fueling gas [5]. Surface analysis shows concentrations of oxygen and carbon typical of metal surfaces with a measured oxide layer thickness of 15 nm at the surface. Standard wall conditioning techniques are employed to reduce water and carbon levels [6]. Baking to 170^o C for ~ 100 hours reduces the partial pressure of water by an order of magnitude. Hydrogen glow discharge cleaning (GDC) for ~ 30 hours during the bake provides a modest reduction of volatile (CH_4 , CO , CO_2) gas species. Helium shot conditioning and titanium gettering further reduce impurities and lead to improved plasma performance.

The performance of spheromaks is sensitive to the plasma density and impurity content since low temperature resistive plasmas have lower confining magnetic fields and corresponding worse confinement than hotter plasmas because currents in the plasma produce the fields. A key measure for the spheromak is the quantity I/N (equivalently j/n), which can be related to the ratio of ohmic heating input power to impurity radiation loss power. When j/n is greater than about 10^{-14} A-m, the ohmic heating will exceed the impurity radiation loss and the electron temperature will be transport limited. The evolution of the density after formation depends on whether the current in the spheromak (as opposed to the injector current) is sustained or is decaying. In sustained spheromaks the density depends strongly on whether the sustaining current is above the spheromak formation threshold, expressed as $\lambda = I/\Psi$, where I is the current and Ψ is initial vacuum magnetic flux threading the injector region. If below threshold, then there is only a weak dependence on λ since most of the current and plasma remain in the injector region. As the current rises above the threshold, the injector plasma is swept out into the main chamber so that the spheromak density can be maintained at a high level.

To prepare for deuterium operation, wall-conditioning techniques were employed in order to exchange the hydrogen-dominated wall with deuterium. Four hours of GDC in D_2 was followed by ~ 100 , short duration, formation only conditioning discharges. The conditioning discharges use only the stored energy in the formation bank (500kJ) so that more discharges can be obtained more rapidly using less energy. The working gas for the conditioning discharges was alternated between helium and D_2 . Helium shot conditioning reduces the production of volatile impurity species pressures by reducing the carbon and oxide layer on the metal surface. In addition to GDC and conditioning discharges, ~ 50 full duration discharges with deuterium fueling were required to reduce the atomic hydrogen gas level by about an order of magnitude.

4. Deuterium plasmas

In SSPX, the fueling gas is puffed into the injector region by eight pulsed gas valves mounted uniformly around the injector on the tapered section of the gun; see Fig. 1. Typically, when fueling with H₂, the gas valves are pulsed ~250 μs before the high voltage is applied. After the high voltage is applied, there is an additional 300 μs delay before breakdown occurs. The combined delay time of 550 μs is the time it takes for the gas (turbulent flow) to spread out into the injector region and satisfy the conditions required for Paschen breakdown. During deuterium operations, the combined gas-puff-to-breakdown delay time increased to ~790 μs. The increased delay time is consistent with isotopic mass scaling of the sound speed.

The expansion time of the plasma out of the injector was determined using 7 equally spaced edge magnetic field probes in the upper half of the flux conserver. The measured time for the injector plasma to reach the midplane (d=40cm) was the same (t=11 μsec) for both the D₂ and H₂ fueled discharges, from which we conclude that the motion of the injected plasma is not inertial (proportional to the Alfvén velocity), but dominated by a force balance between $\mathbf{J} \times \mathbf{B}$ and the injector vacuum fields. Other than the delayed gas time, no other mass effects were observed during the initial formation.

A time history comparing two discharges, one fueled with hydrogen and the other deuterium, is shown in Figure 2. With the exception of the deuterium gas puff timing, as discussed above, the programmed shot parameters (gun flux, bank voltages and fueling pressure) for both discharges are identical. The gun current for the deuterium discharge is ~10% less than the gun current for the hydrogen discharge while both discharges have similar gun voltage and electron density time traces. Since the resistance of the external electrical circuit is constant, the change in gun current and constant gun voltage correlates with an increase in plasma resistivity for the deuterium discharge. Furthermore, the measured edge

poloidal magnetic field for the deuterium discharge is less and is decaying more rapidly, consistent with an increase in plasma resistivity. In subsequent deuterium discharges, to achieve the same injector current and voltage as the hydrogen fueled discharge (shot 9717), more bank energy was required. The increased plasma resistivity and more rapid magnetic field decay time correlates with an increase in impurity radiation for the deuterium discharges.

To characterize the impurity radiation, line emissions in the 100-1600 Å spectral region are measured using an absolutely calibrated SPRED spectrograph [7]. The spectrograph has a tangential view of the magnetic axis through the midplane and provides a time-integrated spectrum of the discharge. As seen in Figure 3, the measured spectrum for the deuterium discharge shows an increase in titanium line emissions while the oxygen line emissions are similar. The increased titanium emissions are attributed to an increase in the sputtering yield of titanium by deuterium ions. At spheromak relevant ion temperatures ($T_i = T_e \sim 150$ eV during sustainment) and sheath voltages (~ 300 V), the sputtering yield of titanium by deuterium is an order of magnitude greater than sputtering by hydrogen ions [8]. Spectroscopic analysis of measured impurity emissions for an ensemble of H_2 and D_2 fueled discharges show a 40% increase in the total radiated energy (J/cm^2) due to an increase in titanium line emissions for the D_2 discharges. Table 1 lists the energy input (E_{input}) to build to the maximum field, the magnetic field energy ($W_B @ t=3ms$), and the radiated energy (E_{rad}) from spectroscopy for D_2 and H_2 discharges with the same E_{input} and a D_2 discharge with increased E_{input} . The D_2 discharge with the same $E_{input}=115kJ$ as the H_2 discharge has less magnetic field energy and more impurity radiated energy. In an attempt to obtain a discharge in D_2 with the same magnetic field energy as the H_2 in Table 1, the input energy was raised from 115kJ to 133kJ. More energy went into the magnetic field, however the E_{rad} also increased due to increased titanium emissions. The decrease in stored magnetic energy for the

deuterium-fueled discharges is attributed to an increase in radiation due to increased titanium emissions.

Measured radial profiles of T_e and n_e , for both deuterium and hydrogen fueled discharges are essentially identical in shape and magnitude. Over one hundred discharges with a peak T_e greater than 100 eV have been averaged to obtain the T_e and n_e profiles shown in Figure 4. The radial profiles are peaked at the magnetic axis and are parabolic in shape. Because confinement time is dominated by the edge power associated with the fields we focus on χ_e , instead of τ_e . The CORSICA calculated core thermal diffusivity, χ_e , is also independent of fueling gas. Figure 5 shows a plot of the calculated core χ_e versus peak T_e . At higher T_e , the magnitude of χ_e is Bohm-like but scaling is different for both H2 and D2 fueled discharges.

5. Summary

On SSPX, progress has been made in understanding both magnetic field generation and confinement, enabling the production of high (~ 1 T) magnetic field spheromaks with core electron temperatures (T_e) of >200 eV and thermal conduction below $\chi_e < 10$ m²/s in the plasma core. To build upon these results, experiments with D₂ fueling were conducted to explore possible further improvement in plasma performance as seen in tokamaks. To obtain the same measured plasma parameters, more input energy was required for the D₂ fueled discharges. Furthermore, the measured edge poloidal magnetic field for deuterium discharges was less and decays more rapidly. The increased input energy and a more rapid magnetic field decay time correlates with an increase in plasma resistivity. Spectroscopic measurements showed a modest increase in titanium line emissions. The increased titanium emissions are attributed to an increase in the sputtering yield of titanium by deuterium ions. With higher input energy, the D₂ fueled discharges show similar results to those with H₂ fueling. Electron temperatures of ~ 200 eV with similar electron densities were observed. Isotope mass effects are not observed on SSPX.

Acknowledgements

This work was carried out under the auspices of US DOE by the University of California Lawrence Livermore National Laboratory under Contract W-7405-ENG-48.

References

1. T. K. Fowler, J. S. Hardwick, T. R. Jarboe, *Comments Plasma Phys. Controll. Fus.* **16** (1994).
2. E. B. Hooper, J. H. Hammer, C. W. Barnes *et al.*, *Fusion Techn.* **29** (1996).
3. E. B. Hooper, L. D. Pearlstein, and R. H. Bulmer, *Nucl. Fusion* **39**, 863 (1999).
4. M. Bessenrodt-Weberpals *et al.*, *Nucl. Fusion* **33**, 1205 (1993).
5. D. A. Buchenauer, B. E. Mills, R. D. Wood *et al.*, *J. Nucl. Mater.* 290-293 (2001) 1165
6. R. D. Wood, *et al.*, *J. Nucl. Mater.* 290-293 (2001) 513
7. R. J. Fonk, A. T. Ramsey, R. V. Yelle, *Appl. Optics* **21**, 2115 (1982).
8. E. W. Thomas, *Atomic Data for Controlled Fusion Research* **3**, (1985) A10.

Figure Captions

Figure 1. SSPX with Corsica equilibrium profile.

Figure 2. Time history of SSPX discharge with hydrogen (black) and deuterium (red); gun current, gun voltage, electron density and midplane edge poloidal field.

Figure 3. Time-integrated spectrum of hydrogen (blue) and deuterium (red) discharge showing increased titanium emissions.

Figure 4. Electron temperature and density profiles comparing hydrogen (circles) and deuterium (diamonds) discharges.

Figure 5. CORSICA calculated thermal diffusivity, χ_e , for hydrogen (circles) and deuterium fueled discharges (diamonds).

Table 1. Energy balance comparison of D₂ and H₂ fueled discharges. E_{rad} is determined from spectroscopy assuming the measured emissions are uniformly distributed over the plasma volume. All values are in kJ.

Table 1. Energy balance comparison of D₂ and H₂ fueled discharges. E_{rad} is determined from spectroscopy assuming the measured emissions are uniformly distributed over the plasma volume. All values are in kJ.

	H2 (9717)	D2 (11628)	D2 (12372)
E _{input} (formation)	115	115	133
W _b (magnetic field)	14	9	12
E _{rad} (impurities)	63	77	98

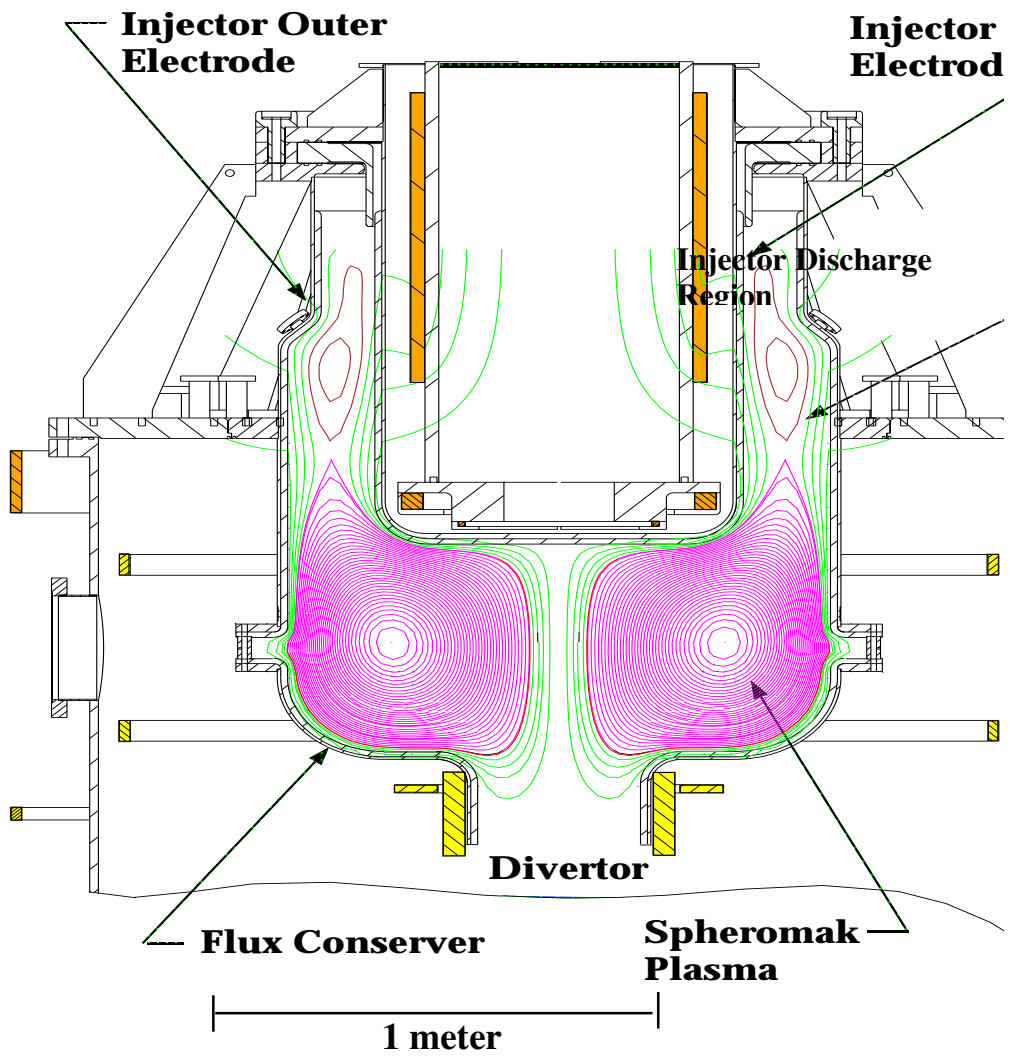


Figure 1. SSPX with Corsica equilibrium profile.

.

Figure 2. Time history of SSPX discharge with hydrogen (black) and deuterium (red); gun current, gun voltage, electron density and midplane edge poloidal field.

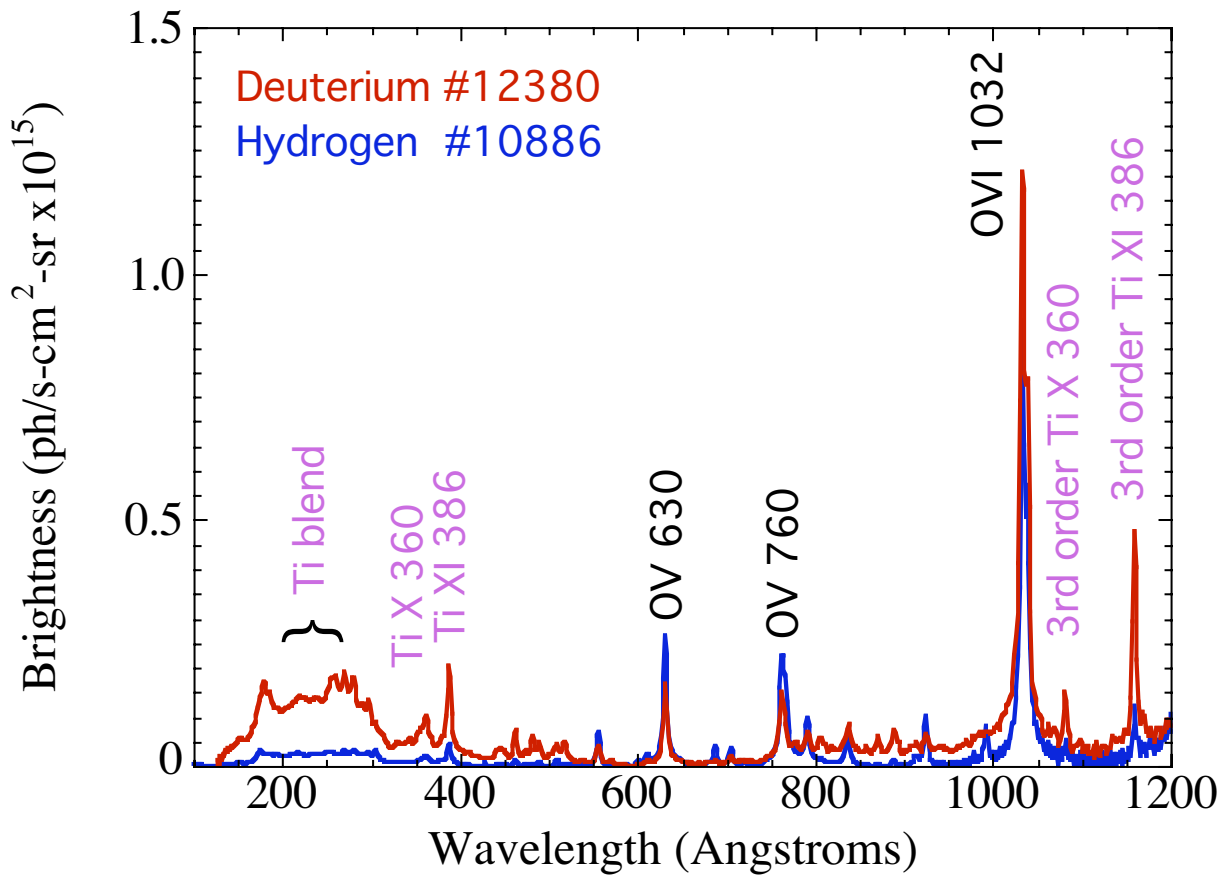


Figure 3. Time-integrated spectrum of hydrogen (blue) and deuterium (red) discharge showing increased titanium emissions.

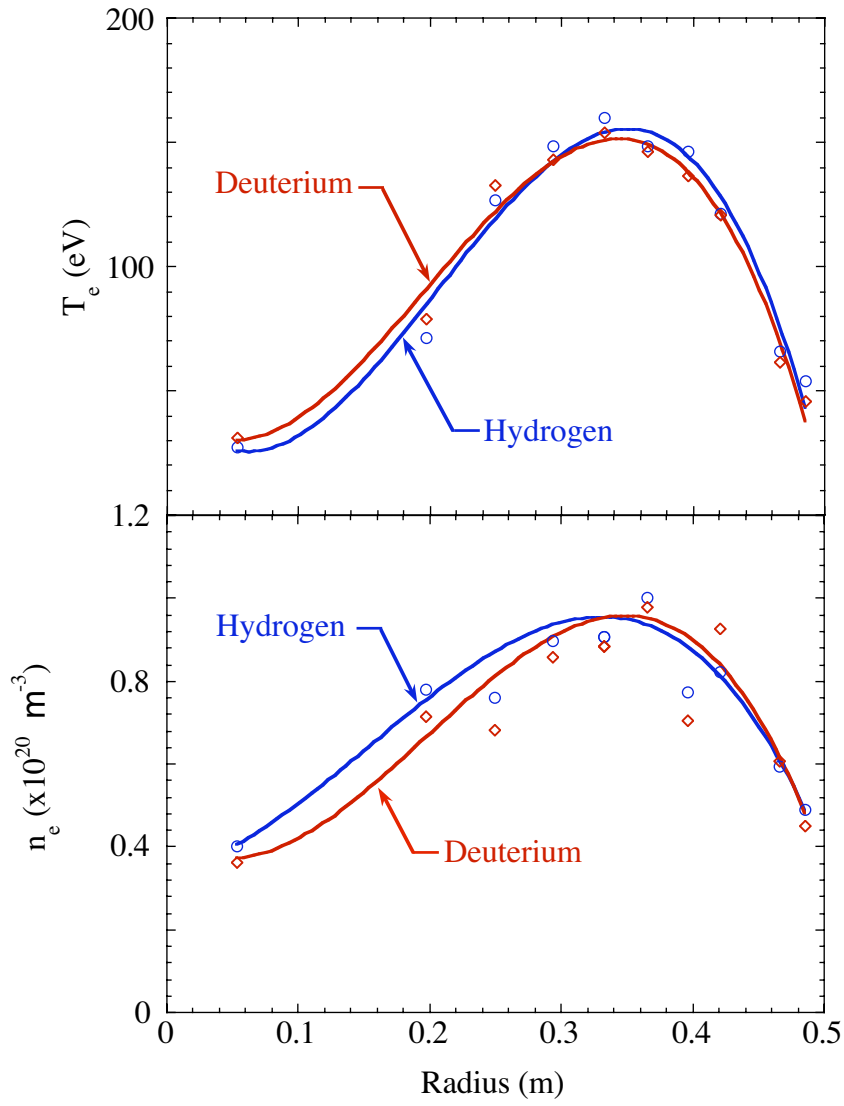


Figure 4. Electron temperature and density profiles comparing hydrogen (circles) and deuterium (diamonds) discharges.

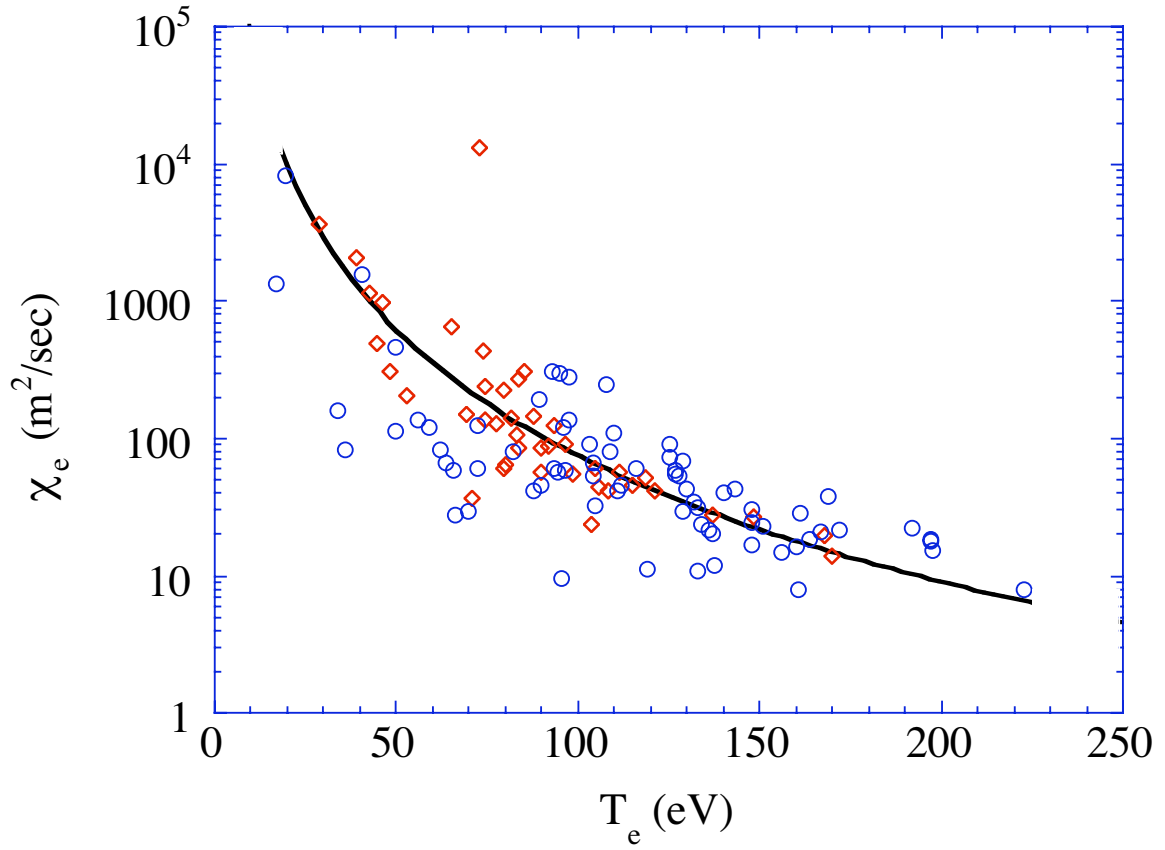


Figure 5. CORSICA calculated thermal diffusivity, χ_e , for hydrogen (circles) and deuterium fueled discharges (diamonds).

University of California
Lawrence Livermore National Laboratory
Technical Information Department
Livermore, CA 94551

